Autotuning of Resonant Magnetic Induction Communications

***Abstract*—The paper presents a novel autotuning scheme to ensure optimal energy transfer using Magnetic Resonance Communication (MRC) in challenging environments such as small networks of implanted intrabody nodes to manage chronic diseases. Our approach employs a control mechanism for capacitive tuning to adaptively maintain resonance and optimal energy transfer. This method compensates for drifts in circuit parameters and external perturbations, ensuring efficient and reliable communication in intrabody networks. Experimental results demonstrate the effectiveness of our autotuning scheme in various simulated scenarios, including step and ramp perturbations in circuit parameters. We show that our approach can significantly improve the efficiency of MRC systems in the face of both the short-term variations and longer term drifts.**

***Index Terms*—Magnetic Induction Communications, Autotuning, Resonance, Q-factor**

I. Introduction

Smart sensing and short-range wireless communications form the bedrock for building sophisticated IoT based automation services for close-range monitoring of various types of activities. Radio frequency (RF) based communications (e.g., Bluetooth, WiFi) are well established and work extremely well in open, uncluttered environments, and are thus the technology of choice for longer range communications through the air. However, increasingly the communications needs involve environments with characteristics that make RF communications difficult – these include presence of aqueous or plant/animal tissue media which cause high signal absorption, metallic clutter that causes diffraction or shielding of the signals, or underground operation that results in an extremely complex communications channel. Reducing absorption by choosing lower RF frequencies helps in attenuation [1], but needs bigger antennas, which introduces the problem of undesirable size and potentially severe interference with nearby radios. Also, the power consumption of RF radios is generally quite high.

Ultrasound communication (USC) is a well established non-RF technology that works well in aqueous and underground media, but requires larger size radios and higher power consumption, but still cannot operate in a cluttered environment. Visible light communication (VLC) is an excellent technology for line-of-sight communications through transparent media, but its performance deteriorates rapidly in the presence of obstacles.

Another well-known short-range non-RF technology is based on the principle of resonant inductive coupling (RIC) between two matched coils, each forming an LC circuit with the same resonance frequency. Magnetic resonance communication (MRC) modulates the magnetic field and forms the basis for near field communications (NFC). Such communication can be made purely magnetic by blocking the electric field (e.g., via an Aluminium foil) and therefore will not suffer from the usual fading and diffraction associated with the electric field. Due to these advantages, MRC has been studied for some RF-challenged environments such as underwater [2], underground [3], etc., and some commercial products are available, such as audio headphones by NXP [4] and RuBee MRC tags useful in product labeling [5].

MRC has been examined in two contexts; (a) monitoring the quality deterioration of fresh-foods while they are being transported or stored during transit [6], and (b) Human Body Communications (HBC) [7]. It has been shown that MRC works better than other HBC technologies such as Capacitive or Galvanic coupling [7] and comparable to ultrasound [8]. It has also been found that MRC is very robust against variations that one would expect in on/in-body environment such as movement, posture, clothing, person to person variations (e.g., build, weight, etc.) [7]. It has been noted that in contrast MRC antennas have been reported to be very sensitive to misalignments [9] and require proper acoustic impedance matching [10].

In the context of HBC, an interesting emerging application of MRC is communications among the nodes of (usually small) networks some of which may be inside the body, while some are on-body. The primary use case for these is the management of chronic diseases that continue to rise rapidly throughout the world due to the rapidly aging population in developed countries and increasing air, water, and food pollution in developing countries. In the US, more than 50% of older adults $\geq$ 3 chronic conditions [11]. According to the US CDC, chronic diseases account for nearly 75% of aggregate healthcare spending, and their treatment accounts for 96% of Medicare costs and 83% of Medicaid costs [12]. Management of chronic diseases, often requires collecting relevant signals (e.g., nerve conduction, muscle activity, blood flow, etc.) from multiple points and their fusion to determine the actuation (drug or electric stimulation delivery). For example, overactive bladder control ideally involves a spinal cord neuro-modulator based on the bladder pressure monitoring by an implantable pressure sensor and the urine volume monitoring by micro-electrode-mediated neural recording [13], [14]. Thus the need for an intra-body network of nodes, communicating via MRC is one of the important scenarios.

A crucial aspect of such intrabody networks is the serious limitations that they face. The nodes should be as small as possible to avoid tissue damage, should last for as long as they are needed (or the lifetime of the patient), and should not require any adjustments/changes. Thus, the wireless power transfer (WPT) to the nodes (along with supercapacitors to hold the charge) is a much more desirable solution than batteries. The energy transfer could occur either from an energy harvesting node inside the body (e.g., close to the

heart or lungs) or supplied from a battery-operated on-body device such as a smart watch. An efficient WPT mechanism is crucial to ensure that the nodes can receive adequate energy supply. Note that even a small 20db path-loss through the body would reduce 1 mW transmitted power to only 10μW on the receiver side. Put another way, 99% of the transmitted power will be wasted or absorbed by the tissue.

Given this backdrop, it is crucial to make MRC based communication and power transfer highly efficient, and keep it so over very long periods of time (e.g., 10's of years) without need for any physical access for the purposes of tuning the circuits. This is the topic that we address in this paper and propose an autotuning scheme to ensure the highest possible energy transfer without any manual intervention.

II. Q Factor and Autotuning

MRC works by energy transfer between a transmit and a receive coil separated by the desired communication distance. Each coil has certain inductance L and connected to a capacitor C in series or in parallel, plus a resistor in series to control the current. At any angular frequency $\omega = 1\pi f$, such a circuit has capacitive and inductive reactances, denoted X_C and X_L respectively, given by $X_C = -1/(j\omega)$ and $X_L = j\omega$. The total impedance of a series RLC circuit is given by

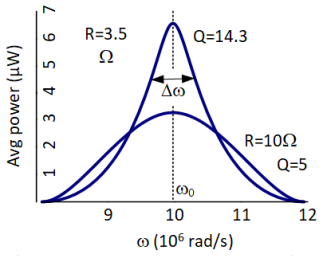

Fig. 1: Resonance Illustration

$$Z = R + j\left(X_L - X_c\right) = R + j\left(\omega L - \frac{1}{\omega C}\right) \quad (1)$$

When $X_L > X_C$ the circuit is *inductive*, whereas $X_C > X_L$ makes the circuit *capacitive*. Electrical resonance occurs in an AC circuit when the inductive and capacitive reactance are equal, i.e.,

$$X_L = X_c, \quad \implies \omega_r L = \frac{1}{\omega_r C}, \quad \implies \omega_r = \frac{1}{\sqrt{LC}} \quad (2)$$

In resonant condition, the impedance of the circuit becomes purely resistive, i.e. $Z = R$.

An important performance indicator of an RLC circuit is the *quality factor* Q, defined as the ratio of the energy stored in the circuit to the energy dissipated by the circuit [15], [16]. It is merely the ratio of reactance and resistance, and is given by $Q = 1/\omega_r RC$).

$$Q = \frac{\text{Energy stored in the circuit per cycle}}{\text{Energy dissipated by the circuit per cycle}} = \frac{\text{Reactance}}{\text{Resistance}} = \frac{X_L\ (\text{or } \mathrm{X_C})}{R} = \frac{\omega_r L}{R} = \frac{1}{R\omega_r C} \quad (3)$$

The quality factor mainly indicates how efficiently inductors and capacitors in the circuit transfer their energy from the source to the load. The quality factor is also defined as the frequency-to-bandwidth ratio of the resonator, i.e.

$$Q = \frac{f_r}{\Delta f} = \frac{\omega_r}{\Delta\omega} \quad (4)$$

where Δf is the resonance width, i.e. the bandwidth over which the power is greater than half the power at the resonant frequency $\Delta\omega$ is the corresponding angular half-power bandwidth(See Fig. 1). From equation(3)-(4) we can observe that the bandwidth of the RLC circuit can be controlled by the resistance only, keeping all the other components same.

The transmit coil can transfer energy to the receive coil because of the mutual inductance between the two coils, denoted M. Thus a time varying voltage V_1 (and corresponding current I_1) in the transmit coil induces a current I_2 in the receiving coil. If the resistor, inductor, and capacitor values of the two coils are (R_1, L_1, C_1) and (R_2, L_2, C_2) respectively, then from Kirchoff's laws, it is easy to conclude that $I_2 = -\frac{j\omega_r M}{R_2} I_1$.

Thus if the transmit data is modulated on the magnetic flux, then the receiver can receive and demodulate the signal. The effectiveness of the mutual coupling is measured by the *coupling coefficient* κ, which can be estimated as

$$\kappa = \frac{M}{\sqrt{L_1 L_2}} \quad (5)$$

If P_1 and P_2 are the transmitted and received power respectively, then the power transfer ratio is given by [16]

$$\frac{P_2}{P_1} = \frac{\omega_r^2 M^2 R_1 R_2}{R_1^2 R_2^2} = \kappa^2 Q_1.Q_2 \quad (6)$$

where Q_1 and Q_2 are the quality factors of the transmit and receive coils respectively. Thus, the power transfer is proportional to the coupling coefficient and the quality factors of the transceiver coils. It is clear that to maximize energy transfer, both Q_1 and Q_2 should be as high as possible. Unfortunately, a high Q value results in a much sharper peak in the resonance curve as shown in Fig. 1. The key problem with the sharp peak is its stability, since a slight change in the parameters or load variations can change the resonance frequency enough to substantially lower the transfer efficiency. In this paper we devise an autotuning mechanism to ensure that any drift is compensated for and thus the energy transfer stays near its peak.

In general, there could be multiple reasons for drift, some significant, some not. For example, the drift in the capacitance due to aging and temperature variations depends on the type of capacitor used. For small capacitances relevant for the resonant LC tank, a class 1 CoG capacitor is ideal, and its aging and temperature related variables are generally quite small or negligible (see https://www.electronics-notes.com/articles/electronic_components/capacitors/ceramic-dielectric-types-c0g-x7r-z5u-y5v.php). However, the mounting of the capacitor on the circuit board and the solder can experience significant changes over time, particularly at higher temperatures [17]. The change could eventually lead to failures; however, our focus here is not failure, but the drift in properties that may occur any time, and certainly much before outright failure.

In addition to the potential drift in the resonance circuit itself, there are other changes whose impact could be perturb the resonance significantly. One source of perturbation is the movement of the transmit or receive coil while it is deployed in the patient. Depending on the location, slight movements and orientation changes occur as the body muscles move. These movements would also change the parasitic capacitance contributed by the the body and its contact with the coils. The net effect of these variation is the change in the resonance circuit parameters and thereby a drop in power delivered to

the load. Another potential source of perturbation concerns the change in physiological parameter of the person such as blood pressure or heart rate, which we investigate in this paper. While very short-term changes (e.g., 1 minute or less) are not relevant for autotuning, it is desirable to respond to longer term changes either to maintain communication quality (when signal attenuation goes below the nominal value) or to save energy by reducing the transmit energy (when the attenuation is lower than the nominal value).

A. Related Work

The problem of "detuning" of resonant circuits due to various impacts has been well recognized and studied in the context of wireless power transfer (WPT). Note that our problem involves integrated WPT and communication which places certain restriction as compared to the pure WPT environment. The main techniques as described below.

The most direct compensation method is to introduce a switchable capacitor/inductor matrix to compensate for the capacitance drift. However, the solutions tend to be rather heavy duty and intended for large power transfer situations. For example, Si et. al. [18] consider power transfer to pacemaker from outside and describe a way of changing frequency of the operation. It includes both capacitor switching and frequency switching to control power transfer. Lim et al. [19] introduce a self-adaptive capacitor matrix with automated searching for configuration with changing distance between transmit and receive coils.

Another method is to adjust the capacitance via pulse-width modulation (PWM) of the input signal to control how much chance the capacitor gets to charge/discharge in each cycle, which effectively changes its capacitance. Porto et al. [20] do this by using an amplifier, and a double-sided version is discussed in [21]. However, such complexity in unwarranted since voltage controlled capacitors, many built in with push-pull circuit are readily available. Furthermore, PWM can interfere with the communication in the integrated power transfer and communications mechanism that we are interested in. Switching the operating frequency to always correspond to the resonant frequency is a popular method explored in several papers. For example, a self-oscillating switching technique was used in [22]. For our application, frequency switching is undesirable as it is complex and requires the receiver to re-latch to the change frequency to enable proper communication. Another method is to control the phase shift on the the receive side by using the semiactive rectifier (SAR) where the trigger modes of the driving signals are altered to achieve matching of the load resistance or reactance. Mai, et al. [23] use both pulse width and the phase shift angle control to provide matching for both the drift and load resistance variations. In our context the rectification will work only for WPT, not communications.

III. Capacitive Tuning

A. Circuit Design

Two RLC circuits for magnetic coupling were designed. The main criteria was to have an efficient energy transfer between the two circuits at a specific frequency (13.56 MHz, which is popularly used for MRC). The values for resistance, inductance and capacitance can be obtained from the resonance frequency and Q factor. The circuits were designed according to the circuit design in [7]. According to [24], to have an optimal energy transfer, the coupling factor (k_{mrc}) needs to be equal to $\frac{1}{\sqrt{Q_r \cdot Q_t}}$. This coupling factor was used in the simulations. The parameter values for the RLC circuit are shown in Table I.

Fig. 2: MRC Coil

B. On-Body Experiments

As shown in equation 6, the efficiency of transmission depends on the Q-factors of the transmitter and receiver and the coupling factor of the medium. In a complex medium such as the human body, it would be naive to assume that the coupling factor would remain constant. We conducted a couple of experiments, in which the transmitter and receiver of a pair of matching circuits on skin was used to measure how the efficiency would change. Two matching circuits were built each with flat circular coils. The coils were placed on the skin of a subject and were shielded magnetically on the top to prevent any signal leakage into the air. The transmit and receive coils were identical and are placed on the left hand arm, 15 centimeters apart. The antenna is shown in Fig. 2. We then conducted several experiment to assess the variability of through-the-body communication channel with respect to some common changes in physiological parameters.

L	9.27 μ H
C	14.86 pf
R	50 Ω
k_{mrc}	0.063

TABLE I: Circuit parameters

1) Skin Temperature vs. Transmission Efficiency: Our first experiment examined the energy transfer variation with respect to the skin temperature. For this, we increased/decreased body temperature in the left arm and measured the efficiency. A common rubber bottle was used as the heating/cooling agent. The bottle was placed on the arm, between the two sensors, removed after 2 minutes to avoid any extended impacts, then the power was measured. The experiments were done at 5 different temperatures, $10°$, $15°$, $27°$, $35°$ and $40°$ Celsius. As can be seen in Fig. 3.a, there is less than 1.78 dB loss between maximum and minimum measured dB loss and there is no apparent correlation between the temperature and efficiency.

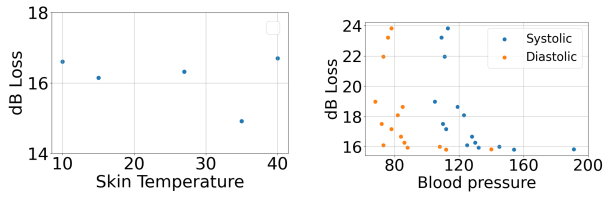

(a) (b)

Fig. 3: a. dB Loss vs. Skin Temperature, b. dB Loss vs. Blood Pressure

2) Blood Pressure vs. Transmission Efficiency: The second experiment was done with blood pressure, where we measured the blood pressure (both Diastolic and Systolic) and efficiency. The measurements were done at different times of the day and after different activities to get a range of numbers covered for BP. As can be seen in Fig. reff:skint.b, there is approximately 8 dB difference between maximum and minimum measured dB loss and it changes rather drastically. Although our experiments may not present a direct correlation between the two, we can see that blood pressure and possibly other body parameters do affect on how efficient the transmission is. Therefore, it is important to compensate for such changes automatically to keep the transmission efficiency high. The proposed control scheme attempts to address this need for adaptation.

C. Proposed Control Scheme

We model the disturbance in the transmission as a perturbation in the capacitance of the transmitter and/or the receiver. The compensation for these perturbations can be used to control the Q-factor and the resonance frequency (and hence the coupling factor according to equation 6). The control of the capacitance can be easily swapped with that of the inductance, however, a change in inductance is generally more difficult to implement. Controlling the resistor however, would not be a viable option since with resistor control, we can only manage the Q-factor, not the resonant frequency. Capacitance is selected because of its capacity to affect satisfying both objectives, achieving high Q-factor and resonance.

We exploit the fact that the current in the receiver circuit goes down whenever the two circuits do not resonate. So the key part of the controller is that it should find out which part of the slope we are on. The controller only observes the current and whenever the current is not at its peak, the controller is activated. Upon activation, the controller adjusts the capacitance in the positive or negative direction and measures the current after each action. When increased/decreased, if the current is higher than the current measured before activation, the controller keeps selecting the same action. Otherwise, the controller changes direction, meaning that if it was increasing the capacitance until now, it starts decreasing the capacitance, and vice versa, as shown in Algorithm I. The main assumption for the proposed controller is that when it is the transmit side's turn to tune its circuit, the receive side shares its observed current value with the transmit side, assuming that there is a communication between the two circuits.

To design the controller, a truth table is constructed for the controller's behavior based on the following equations:

$$\delta = Sign(C_{t-1} - C_{t-2}) \tag{7}$$

$$\Delta_1 = Sign(I_t - I_{t-1}) \tag{8}$$

$$\Delta_2 = Sign(I_{t-1} - I_{t-2}) \tag{9}$$

Fig. 4.b illustrates the two scenarios of the truth tables. The action means the direction of the step (or sign of the step) that the controller should decide to take.

In Fig. 4.b, the horizontal orange line is used to show the optimal value of capacitance. The controller acts in every scenario according to three data flows it receives, current and action from one time sample before, current and action from two time samples before, and the time. For the receive side, it is a matter of recording the data it already observed, and for the transmit side, this data is sent from the receive side. The controller algorithm I is designed from the truth table show in Fig. 4.b.

Alg. I: Adaptive Step Controller Pseudocode

Observations:
I_t := Receiver Current at time t; I_{t-1} := Receiver Current at time t-1
I_{t-2} := Receiver Current at time t-2; C_{t-1} := Capacitance at time t-1
C_{t-2} := Capacitance at time t-2
Parameters:
W' := Initialization weight; W := Weight; ϵ := Threshold
Δ := Step size; α := Control Action; $\delta = Sign(C_{t-1} - C_{t-2})$
$\Delta_1 = Sign(I_t - I_{t-1})$; $\Delta_2 = Sign(I_{t-1} - I_{t-2})$
If NOT Controller's Turn **Then** $C_t \leftarrow C_{t-1}$
Else {
  If $|I_t - I_{ref}| < \epsilon$ **Then** $C_t \leftarrow C_{t-1}$
  Else {
    if t=1 (First round) **Then** *Initialization* $C_t \leftarrow C_{t-1} + W'\Delta$
    Else {
      if $\epsilon \leq |I_t - I_{ref}| < 2\epsilon$ **Then** $C_t \leftarrow C_{t-1} + W^t \cdot \alpha \cdot \Delta$
      Else {
        If $2\epsilon \leq |I_t - I_{ref}| < 4\epsilon$ **Then**
        $C_t \leftarrow C_{t-1} + 2W^t \cdot \alpha \cdot \Delta$
        Else $C_t \leftarrow C_{t-1} + 4W^t \cdot \alpha \cdot \Delta$
}}}}

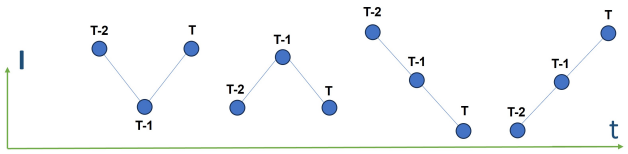

(a) Current Trajectory

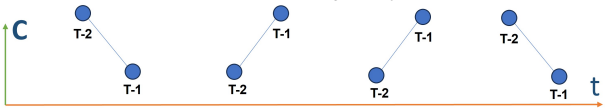

δ	-1	+1	+1	-1
Action	-1	-1	-1	-1
Δ1	+1	-1	-1	+1
Δ2	-1	+1	-1	+1

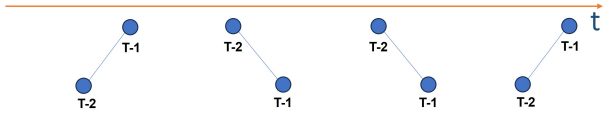

δ	+1	-1	-1	+1
Action	+1	+1	+1	+1
Δ1	+1	-1	-1	+1
Δ2	-1	+1	-1	+1

(b) Capacitance Trajectory

Fig. 4: Controller Truth Table

At first, a one-sided control scheme was investigated, in which only the transmitter has the controller implemented on it. Thus, regardless of which side the perturbation is on, the controller would only be able to tune the circuit on the transmit side. As seen in Table II, this scenario was implemented with 5% perturbation on the receiver side and the controller residing on the transmit side. In this table, the optimal value is obtained by manually changing the

capacitance and finding the optimal value. Using such a mechanism, we can recover only 1% of the perturbation.

5(%) increase	I_{out}(mA)	P_{out}(mW)	Eff(%)
Before control	6.62	2.19	36.3
After control	6.84	2.34	37.4
Optimal values	6.85	2.35	37.5

Table II: Performance of the transmitter side controller in 5% increase perturbation on Receiver side

This means that using a one-side control scheme cannot recover the perturbation that might happen on the other side. Thus having controllers on both the transmit and receive sides should be investigated.

D. Dual Controller Design

Since there are two controllers, on both the transmitter and receiver side, the operation of each controller should be scheduled to prevent any interference. Each controller is given a time interval to act, in which the controller figures out whether it should turn on and the direction it needs to act. In each interval, the controller starts by checking the current. If it is less than the reference by more than the amount of ϵ, the controller's first action is to implement an initial increase in the capacitor. Using this initialization the controller figures out which direction to select using the truth table shown in Figure 4. A decreasing weight is given to each action the controller wants to implement in capacitance to keep the action selection convergent.

We implemented two controllers, a fixed step (FS) controller which only uses one fixed step size, and the adaptive step (AS) controller which uses three steps according to how much current loss has happened. Two main scenarios are investigated: In the first scenario, the perturbation is modeled as a trapezoid (Step Scenario), which starts and ends on both the transmitter and receiver sides. In the second scenario, the perturbation is modeled as a saturating ramp (Ramp Scenario), which starts slowly but never ends but saturates and also happens on both the transmitter and receiver sides. Perturbation in both scenarios is shown in Fig. reffig:drift.

We have done this evaluation using simulations, which are all done using MATLAB SIMULINK toolbox [25]. In all the simulations, activation threshold ϵ and step size are set as $1e^{-8}A$ and $2e^{-17}F$ for the fixed step controller. For the adaptive step controller, these parameters are set as $1e^{-6}A$ and $\{1e^{-17}, 2e^{-17}, 4e^{-17}\}$ F, respectively. Circuit parameters are set initially as shown in Table I. and the voltage source is set to 1 Volt with a frequency 13.56 MHz.

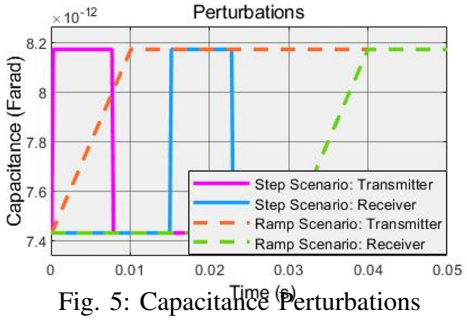

Fig. 5: Capacitance Perturbations

	Without Control	Fixed step	Adaptive step
Scenario 1	34.62%	47%	49.54%
Scenario 2	29.33%	48%	49.78%

Table III: Transmission Efficiency

Step Scenario: The perturbation has been modeled by a trapezoid with height equal to 5 % of capacitance. The proposed controller adapts to the Perturbation according to the step size. The performance of the fixed and adaptive controller can be seen in Figs. 6 and 7. The fixed step controller recovers over 96 % and Adaptive step controller recovers over 99 % of the maximum power. Although the controller uses a very simple and energy-efficient control strategy, FS and AS always settle in the range of 4 % and 0.7 % of the desired capacitance, respectively.

As for the efficiency, after convergence, at worst, FS experienced 47% and AS experienced 49.54% efficiency (as opposed to the ideal 50% efficiency). As shown in the Figs. 6 and 7, four valleys are labeled as A,B,C and D. A is the beginning of trapezoid perturbation (start of the ramp) on the transmitter side, B is the ending of the perturbation (reverting to the original capacitance value) on the transmitter side, C is the beginning of trapezoid perturbation on the receiver side and D is the ending of the perturbation on receiver side. As it can be seen in Fig. 6(b), the efficiency drop is deeper in C and D. The reason is that perturbations on the receiver side have a much deeper effect on the whole system than the perturbations on the transmit side. Note that the uncontrolled case would have resulted in 34.87% efficiency.

Ramp Scenario: Here the perturbation is modeled by a saturating ramp with a maximum equal to 5% of capacitance. Perturbation on the transmit side starts from $1.1e^{-4}$secs, saturating at $1.1e^{-3}$secs, and perturbation on the receive side starts from $3e^{-3}$sec saturating at $4e^{-3}$secs. Fig. 8 shows the performance of the controller in this scenario. FS controller recovers over 98% and AS recovers over 99% of the maximum power. Using this energy-efficient control strategy, FS and AS always settle in the range of 3 % and 0.7 % of the desired capacitance, respectively. As for the efficiency, after convergence, at worst FS and AS experienced 48% and 49.78% efficiency when converged respectively, in contrast to the 29.33% that would have happened in the uncontrolled case. The controllers manage to find a new resonant frequency very quickly without sacrificing much efficiency and power. Since the perturbation is modeled as a saturating ramp, the valleys that were seen in the step scenario, are not present here. However, some fluctuations are completely because the controllers are focused on finding a new resonant frequency independently between each other and hence, missing the optimal efficiency.

Table IV shows the results from actual experiments done using the circuits we designed (with different capacitances). Each experiment was done three times. Each time the temperature and blood pressure were measured to make sure they did not have any effect on the experiment. The experiments show the same trend concerning matching and non-matching circuits. The experiments show less received power which can be due to absorption of power by the body parts and power leaking to the air. Also, the coupling factor can

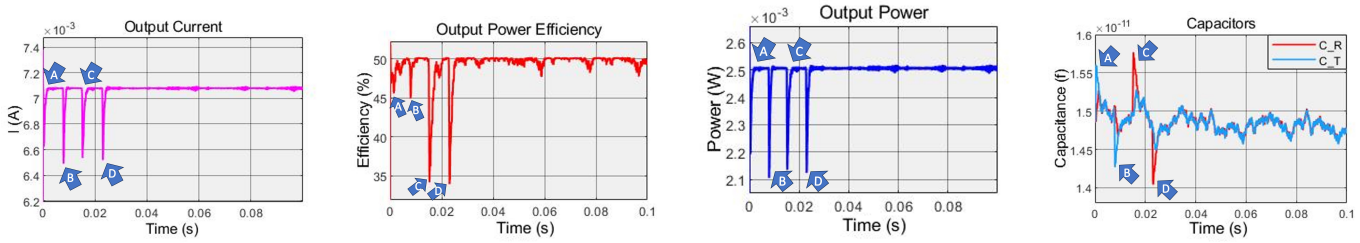

(a) (b) (c) (d)

Fig. 6: **Step Scenario**: Fixed Step Controller Performance a. Output current, b. Efficiency, c. Output power, d. Receiver and transmitter capacitances

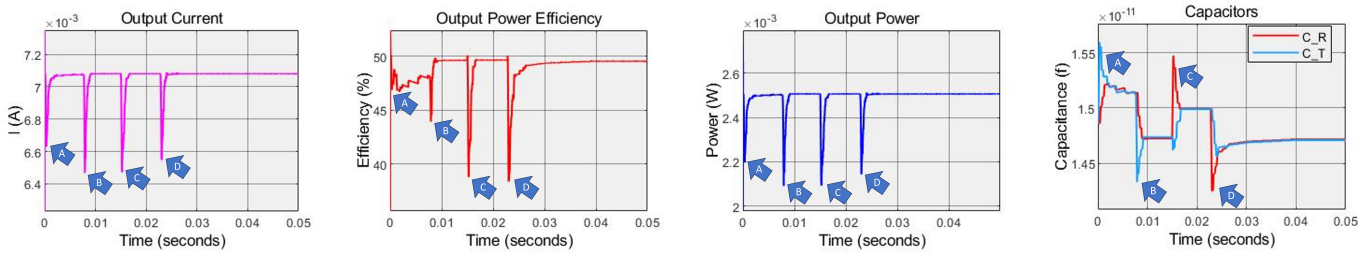

(a) (b) (c) (d)

Fig. 7: **Step Scenario**: Adaptive Step Controller Performance: a. Output current, b. Efficiency, c. Output power, d. Receiver and transmitter capacitances

be approximated to be 0.0495, as opposed to the optimal coupling factor calculated as 0.063 in Table I.

	Receiver Capacitance	
Transmitter Capacitance	C	1.67C
C	42.76%	25.32%
1.67C	31.46%	39.68%

Table IV: Circuit Efficiency in On-body Experiments

IV. Discussion

A. *Controller Performance*

The proposed Adaptive Step (AS) controller acts much better than the Fixed Step (FS) controller since it has the freedom to choose how aggressively it can behave. The sharp drops in current and power in the step scenario are because the perturbation pushes the circuit off the optimum rather sharply. However, the controller can bring it back to a near-optimal state. As it is observed in the ramp scenario, such drops are not experienced in current and power because the mechanism can compensate for the slow changes. The controller can be very fast in balancing the capacitors. The speed is dependent on the activation threshold ϵ and step size. Of course, the speed would play as an adversary to the energy efficiency of the controller and the tradeoff can be studied before implementation.

In the Fixed Step, since the controllers act on both the transmitter and receiver sides but do not share their actions, the capacitance might not settle on a single value (although its change is bounded). Interestingly, even in that case, the efficiency remains high due to the tracking behavior of the controllers. They both keep tracking the optimal value and the other controllers' value, hence what we achieve might not be the exact optimal value, but the near optimal value and more importantly, resonance in the frequency.

One interesting observation about the difference between Fixed and Adaptive controllers is in their behavior in finding the capacitance value corresponding to the maximum power transfer. As can be seen in Fig. 6.d, the Fixed controller behaves erratically even after reaching the optimal value and as a result, it cannot converge. The reason is that the controllers on transmit and receive sides are not communicating. The controller on one side decides to move towards a direction, and ultimately missing on the optima even for a bit, then the other controller overcorrects, which results in a tail-chasing behavior. In contrast, the adaptive Step controller has the option of changing the step size, hence resting at some near optimal value. The activation threshold and step size are hyperparameters of the controller which need to be selected carefully. A lower activation threshold makes the controller more sensitive to how much current loss is and hence the controller would operate more often. A higher activation threshold makes the controller indifferent concerning how much we can recover from the non-optimal states.

The main assumption in the proposed controller is that the observable state for both controllers is the received current. That is, the controller schedule includes the communication back from the receiver to the transmitter, which is a reasonable assumption since the control is essential only when there is communication. In this setting, it is reasonable to assume that the controllers on transmit and receive side are working on the same clock. However, since there is a scheduled communication and controller operation, the controllers are always working according to the schedule and each other, hence this assumption can be easily removed.

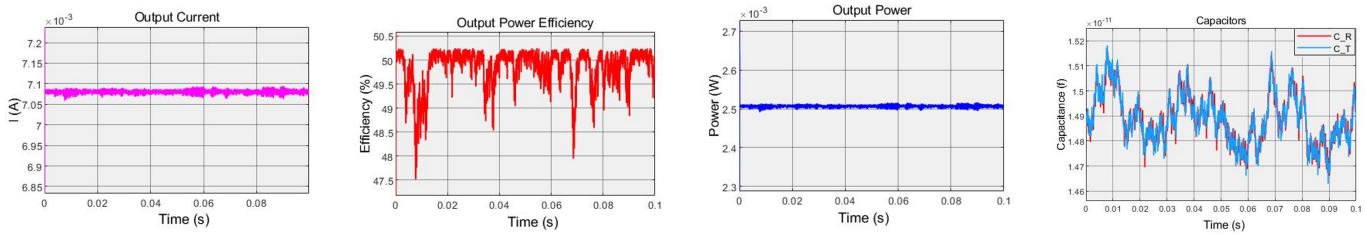

(a) (b) (c) (d)

Fig. 8: **Ramp Scenario**: Fixed Step Controller Performance: a. Output current, b. Efficiency, c. Output power, d. Receiver and transmitter capacitances

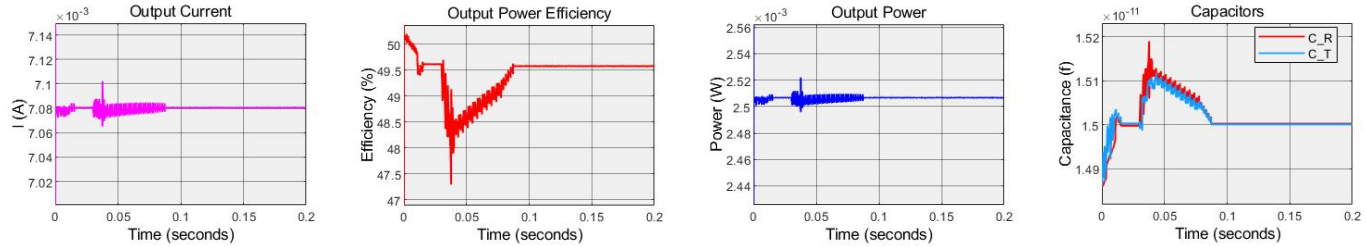

(a) (b) (c) (d)

Fig. 9: **Ramp Scenario**: Adaptive Step Controller Performance: a. Output current, b. Efficiency, c. Output power, d. Receiver and transmitter capacitances

B. In-body Network

As we have shown it in the cartoon diagram in Fig. 10, some body properties change over time (creating a time series) which would, in turn, change the properties of the magnetic communications (improving or worsening it) at the circuit level. The controller would only see the circuit level (received current and power are the observations of the controller), hence no matter how complex the body properties and circuit variables are, it would not matter to the controller at all. If we can obtain a model that translates body properties to circuit variables, it can be exploited to make the controllers have a more efficient connection.

Temporary fluctuations in body properties or the induced current might result in the controller chasing less important spikes. The controller needs to have a mechanism that would mitigate the effect of temporary fluctuations to find out the seasonal trends. A moving average scheme can track the overall behavior of the time series and compensate for long-term weaknesses in the transmission. This would result in an energy-efficient tuning scheme.

We propose using 3 stages for each controller as it is shown in Fig. 11. In the first stage, the controller observes but does not calculate the control signal. In the second stage, the controller observes and implements the control signal. In the final stage, the controller turns off and passes the torch to the other controller. The reason why an observation phase is proposed, is for the controller to calculate an average of the time series, before implementing the control scheme. This would drive the system into mitigating the effect of temporary behaviors and focus on long-term trends.

One interesting extension is to learn the transmission change schedule. One could add a module that tracks the daily or seasonal changes in the medium and translates it to the amount of change in the transmission, so that one can

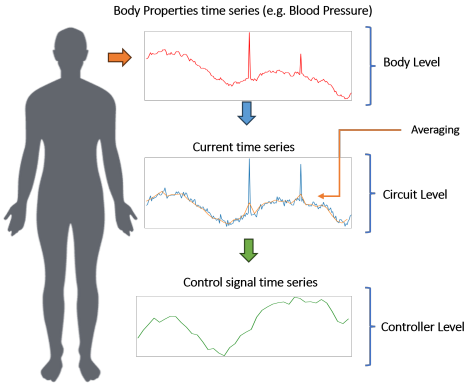

Fig. 10: Cartoon of the controller scheme

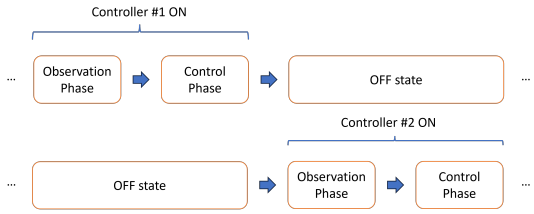

Fig. 11: Scheduling between controllers

have a routine trajectory for the controller to track every day. This should be workable since the day-to-day changes are not expected to have very different characteristics.

According to Fig. 3.b, it can be inferred that the higher values of blood pressure correspond to a lower communication loss. Since older age is generally related to higher blood pressure [26], over the years because of the natural tuning caused by the body, the controller's functionality is expected to improve. This means that the proposed controller is more essential in younger patients who on average have

lower blood pressure. In patients with chronic illnesses, the controller would rely on natural tuning and will require less and less artificial tuning as the patient gets older and hence, it will become more and more efficient.

V. Conclusions

The Magnetic Resonance Communication (MRC) based intrabody networks require high signal and power transfer efficiencies. This, in turn, requires maintaining a high value of the quality factor (QF). Unfortunately, a high QF results in a highly peaked response, so that small drifts can substantially reduce the transfer gain. To address this, we introduced an autotuning scheme that can main high gain automatically in spite of parameter drifts on the transmitter or receiver side and change in channel characteristics. The implications of this research are far-reaching, with potential applications in advanced medical monitoring and treatment strategies. In the future, we will explore the integration of power transfer and communications for intrabody networks with potentially different drifts in different parts of the body, which requires a more elaborate turning and coordination procedure.

References

[1] R. Jedermann *et al.*, "Communication techniques and challenges for wireless food quality monitoring," *Philosophical Transactions of the Royal Society*, vol. 372, no. 2017, p. 20130304, 2014.

[2] I. F. Akyildiz *et al.*, "Realizing underwater communication through magnetic induction," *IEEE Communications Magazine*, vol. 53, no. 11, pp. 42–48, 2015.

[3] Z. Sun *et al.*, "Magnetic induction communications for wireless underground sensor networks," *IEEE Transactions on Antennas and Propagation*, vol. 58, no. 7, pp. 2426–2435, 2010.

[4] "NXP Introduces Ultra-low Power Radio Transceiver Enabling Wireless Earbuds," http://www.everythingrf.com/News/details/1399-nxp-introduces-ultra-low-power-radio-transceiver-enabling-wireless-earbuds.

[5] http://ru-bee.com/.

[6] A. Pal and K. Kant, "Nfmi: Near field magnetic induction basedcommunication," *Elsevier Computer Networks*, Nov 2020.

[7] S. Islam, R. K. Gulati, M. Domic, A. Pal, K. Kant, and A. Kim, "Performance evaluation of magnetic resonance coupling method for intrabody network (ibnet)," *IEEE Transactions on Biomedical Engineering*, vol. 69, no. 6, pp. 1901–1908, June 2022.

[8] R. Gulati, K. Kant, and A. Pal, "Ultrasonic vs. magnetic resonance communication for mixed wearable and implanted devices," *Proc. of IEEE International Conf. on Communications (ICC)*, pp. 5304–5309, May 2022.

[9] A. Ibrahim, M. Meng, and M. Kiani, "A comprehensive comparative study on inductive and ultrasonic wireless power transmission to biomedical implants," *IEEE sensors journal*, vol. 18, no. 9, pp. 3813–3826, 2018.

[10] T. C. Chang, M. J. Weber, M. L. Wang, J. Charthad, B. P. T. Khuri-Yakub, and A. Arbabian, "Design of Tunable Ultrasonic Receivers for Efficient Powering of Implantable Medical Devices With Reconfigurable Power Loads," *IEEE Transactions on Ultrasonics, Ferroelectrics, and Frequency Control*, vol. 63, no. 10, pp. 1554–1562, Oct. 2016. [Online]. Available: http://ieeexplore.ieee.org/document/7562528/

[11] A. Tinker, "How to improve patient outcomes for chronic diseases and comorbidities," http://www.healthcatalyst.com/wp-content/uploads/2014/04/How-to-Improve-Patient-Outcomes.pdf, 2017.

[12] L. P. Fried, "America's health and health care depend on preventing chronic disease," https://www.huffingtonpost.com/entry/americas-health-and-healthcare-depends-on-preventing_us_58c0649de4b070e55af9eade, March 2017.

[13] C. Powell, "Conditional electrical stimulation in animal and human models for neurogenic bladder: working toward a neuroprosthesis," *Current bladder dysfunction reports*, vol. 11, no. 4, pp. 379–385, 2016.

[14] A. Mendez, M. Sawan, T. Minagawa, and J.-J. Wyndaele, "Estimation of bladder volume from afferent neural activity," *IEEE Transactions on Neural Systems and Rehabilitation Engineering*, vol. 21, no. 5, pp. 704–715, 2013.

[15] J. I. Agbinya, *Principles of Inductive Near Field Communications for Internet of Things*. Wharton, TX, USA: River Publishers, 2011.

[16] M. Masihpour, "Cooperative communication in near field magnetic induction communication systems," Ph.D. dissertation, University of Technology, Sydney, 2012.

[17] N. Jiang, L. Zhang, Z.-Q. Liu, L. Sun, W.-M. Long, P. He, M.-Y. Xiong, and M. Zhao, "Reliability issues of lead-free solder joints in electronic devices," *Science and technology of advanced materials*, vol. 20, no. 1, pp. 876–901, 2019.

[18] P. Si, A. P. Hu, S. Malpas, and D. Budgett, "A frequency control method for regulating wireless power to implantable devices," *IEEE transactions on biomedical circuits and systems*, vol. 2, no. 1, pp. 22–29, 2008.

[19] Y. Lim, H. Tang, S. Lim, and J. Park, "An adaptive impedance-matching network based on a novel capacitor matrix for wireless power transfer," *IEEE Transactions on Power Electronics*, vol. 29, no. 8, pp. 4403–4413, 2013.

[20] R. W. Porto, V. J. Brusamarello, L. A. Pereira, and F. R. de Sousa, "Fine tuning of an inductive link through a voltage-controlled capacitance," *IEEE Transactions on Power Electronics*, vol. 32, no. 5, pp. 4115–4124, 2016.

[21] W. Li, G. Wei, C. Cui, X. Zhang, and Q. Zhang, "A double-side self-tuning lcc/s system using a variable switched capacitor based on parameter recognition," *IEEE Transactions on Industrial Electronics*, vol. 68, no. 4, pp. 3069–3078, 2020.

[22] A. Namadmalan, "Self-oscillating tuning loops for series resonant inductive power transfer systems," *IEEE Transactions on Power Electronics*, vol. 31, no. 10, pp. 7320–7327, 2015.

[23] R. Mai, Y. Liu, Y. Li, P. Yue, G. Cao, and Z. He, "An active-rectifier-based maximum efficiency tracking method using an additional measurement coil for wireless power transfer," *IEEE Transactions on Power Electronics*, vol. 33, no. 1, pp. 716–728, 2017.

[24] J. Van Mulders, D. Delabie, C. Lecluyse, C. Buyle, G. Callebaut, L. Van der Perre, and L. De Strycker, "Wireless power transfer: Systems, circuits, standards, and use cases," *Sensors*, vol. 22, no. 15, p. 5573, 2022.

[25] MATLAB, *version: R2019b*. Natick, Massachusetts: The MathWorks Inc., 2019.

[26] J. M. Kotchen, H. E. McKean, and T. A. Kotchen, "Blood pressure trends with aging." *Hypertension*, vol. 4, no. 5_pt_2, p. III128, 1982.